Supporting Information

Photocatalytic degradation of different antibiotics by TiO_2-carbon composites: a case study of tetracycline and ciprofloxacin

Chengyue Tian [a], Wenyu Huang [a, d, *], Zishen Wei [a], Chen Liang [a], Yiwu Dong [a], Ji Shi [c], Xinyun Zhang [a], Guoyou Nong [a], Shuangfei Wang [b, d], Jing Xu [e]

[a] School of Resources, Environment and Materials, Guangxi University, Nanning, 530004, China

[b] School of Light Industry and Food Engineering, Guangxi University, Nanning, 530004, China

[c] School of chemistry and chemical engineering, Guangxi Minzu University, Nanning, 530006, China

[d] Guangxi Bossco Environmental Protection Technology Co.,Ltd, Nanning, 530007, China

[e] State Key Laboratory of Water Resources and Hydropower Engineering Science, Wuhan University, Wuhan, 430072, China

List of Supporting Information

Texts

Tables

Figures

Text S1 Materials

Bagasse (Sugar Mill, Guangxi, China), titanium butoxide (AR), ciprofloxacin (AR), tetracycline (AR), and triethylene diamine (DABCO, AR) were provided by Macklin. Ethanol (AR) was provided by KESHI. Methanol (HPLC) and acetonitrile (HPLC) were provided by Fisher Chemical. Potassium bromate (AR), sodium sulfate anhydrous (AR), tert-Butyl alcohol (TBA, AR), ethylenediaminetetraacetic acid disodium salt (EDTA-2Na, AR), oxalic acid dihydrate (AR), phosphoric acid (HPLC) were respectively provided by several chemical plants, Tianjin, China. Ultrapure water obtained with Milli-Q® equipment was used in this study.

Text S2 Synthesis of photocatalysts

2 g bagasse, 100 mL ultrapure water, and 10 mL absolute ethanol were added to a 500 mL beaker, the bagasse was filtered after sonication for 20 min, 150 mL ultrapure water, and 60 mL absolute ethanol, and placed on a magnetic stirrer. While vigorously stirring, 6 mL of titanium butoxide was added dropwise within 4 min, and then stirring vigorously for 30 min, the agitated bagasse and part of the solution were poured into a 100 mL Teflon-lined stainless steel autoclave and hydrothermally heated at 160°C for 24 h. After the hydrothermal material was suction filtered and rinsed three times with water and ethanol, it was moved to an oven for drying at 80°C. The dried material was transferred to a corundum boat, kept in a tube furnace (with hydrogen-argon mixture) at 400°C for 3 h (heating rate 10°C/min), and then cooled down naturally. The obtained material was named H_2/T-BC.

Add 150 mL ultrapure water and 60 mL absolute ethanol, and place on a magnetic stirrer. While vigorously stirring, 6 mL of titanium butoxide was added dropwise within 4 min, after stirring vigorously for 30 min, the part of the solution was poured into a 100 mL Teflon-lined stainless steel autoclave and hydrothermally heated at 160°C for 24 h. After the hydrothermal material was suction filtered and rinsed three times with water and ethanol, it was moved to an oven for drying at 80°C. The dried material was moved into a corundum boat, kept in a tube furnace (with hydrogen-argon mixture) at 400°C for 3 h (heating rate 10°C/min), and then cooled down naturally. The obtained material was named H_2/T.

2 g bagasse, 100 mL ultrapure water, and 10 mL absolute ethanol were added to a 500 mL beaker, the bagasse was filtered off after sonicating for 20 min, 150 mL ultrapure water and 60 mL absolute ethanol, and placed on a magnetic stirrer. After stirring vigorously for 30 min, the stirred bagasse and a portion of the solution were transferred to a 100 mL Teflon-lined stainless steel autoclave and hydrothermally heated at 160°C for 24 h. After the hydrothermal material was suction filtered and rinsed three times with water and ethanol, it was transferred to an oven for drying at 80°C. The dried material was moved into a corundum boat, kept in a tube furnace (with hydrogen-argon mixture) at 400°C for 3 h (heating rate 10°C/min), and then cooled down naturally. The obtained material was named H_2/BC.

Text S3 Characterization and Photoelectrochemical measurements

Scanning electron microscopy (SEM), energy dispersive spectrometer (EDS), and high-resolution transmission electron microscope (HRTEM) were performed on Zeiss Sigma 300, smartedx, and JEOL JEM-2800. The X-ray

diffraction (XRD) patterns of the samples were obtained using Bruker D8 Discover in the 2θ range of 5-90° and at a scan rate of 5°/min (Cu Kα source irradiation). Fourier transform infrared spectrometer (FTIR) was performed on Shimadzu IRTracer-100 (400 - 400nm). X-ray photoelectron spectroscopy (XPS) was performed using Thermo Scientific K-Alpha with an anode of Al Kα radiation (1486.6 eV) X-ray sources. UV-vis diffuse reflectance spectra (UV-vis DRS) were obtained with Shimadzu UV-3600Plus. Wavelength: 200 – 1000 nm. Tauc plot is mainly based on the formula proposed by Tauc, Davis and Mott et al.[1]: $(\alpha hv)^{1/n} = B(hv-Eg)$, where α is absorption coefficient, h is Planck-constant, ν is frequency, B is constant, Eg is the bandgap width of semiconductor, Exponential n is directly related to the type of semiconductor, direct bandgap n=1/2, indirect bandgap n=2. The type of transitions of H_2/T and H_2/T-BC are indirect, n=2. The surface charge (Zeta) was measured using zeta potential analyzer (NanoBrook Omni, Brookhaven, US). The measurements of Mott-Schottky plot (M-S), transient photocurrent (I-t), and electrochemical impedance spectroscope (EIS) were performed using electrochemical workstation (Chenhua, CHI760E China).

The sample preparation method is as follows.

SEM: An appropriate amount of H_2/BC and H_2/T-BC was glued onto the conductive adhesive and sprayed with gold for 45 s (platinum target) using an Oxford Quorum SC7620 sputtering coater at 10 mA. TEM: An appropriate amount of H_2/T-BC was taken for sample preparation using a copper mesh (microgrid carbon film). XRD: H_2/T, H_2/BC, and H_2/T-BC were milled and pressed separately. FTIR: H_2/T, H_2/BC, and H_2/T-BC were mixed and ground separately with potassium bromide, and the ratio of sample to potassium bromide was approximately 1: 100. XPS: H_2/BC and H_2/T-BC were pressed separately and attached to the sample disk. UV-vis DRS: powder samples diluted with a non-absorbing material ($BaSO_4$). Zeta: An equal amount of H_2/T-BC was weighed and transferred into a 50 mL cuvette, diluted with water and adjusted to pH 2, 4, 5, 7, 8 and 10 respectively. Ultrasonication was used to make the material fully dispersed in the solution, and after a period of natural settling, the supernatant was taken for determination. M-S, I-t, and EIS: Weigh 10 mg of H_2/T, H_2/T-BC powder samples were dispersed in 1 mL of ethanol, then add 20 µL of 5 % Nafion ethanol solution, sonicate for 30 min to form a suspension and then dispersed and coated on ITO substrate for drying.

Text S4 Photocatalytic activity

Conditions for TC determination: Mobile phase was V (0.01 mol/L oxalic acid): V (acetonitrile): V (methanol) = 7:2:1, flow rate of 0.35 mL/min, detection wavelength of 355 nm

Conditions for CIP determination: Mobile phase was V (0.025% phosphoric acid): V (acetonitrile)=87:13, the phosphoric acid solution was prepared and adjusted to pH=3 with triethylamine, flow rate of 0.35 mL/min, detection wavelength of 278 nm.

Text S5 XPS

The C 1s spectrum of H_2/BC was fitted with three peaks. The peak at 284.73 eV was attributed to the C-C bonds (adventitious carbon) [2], which were common in biochar. The peaks at 285.57 eV and 289.19 eV were attributed

to the C-O bonds [2] and COOH/C=O bonds [3], respectively. The O 1s spectrum of H_2/BC can be fitted with two peaks at 531.83 eV and 533.21 eV, which were attributed to C-O bonds [2] and C=O bonds [4], respectively.

Text S6 Zeta

The isoelectric point of TiO_2 was at 6.2 [5, 6], which showed that TiO_2 had a positively charged surface at pH < 6.2 and a negatively charged surface at pH > 6.2. The isoelectric point of bagasse ranged from 2.3 to 6.1 [7-10].

Tab. S1. Fukui calculation results of TC molecular.

Atoms	$f^-(e)$	$f^+(e)$	$f^0(e)$	Atoms	$f^-(e)$	$f^+(e)$	$f^0(e)$
C1	0.0397	0.0303	0.035	C22	0.0038	0.0055	0.0046
C6	0.0497	0.0199	0.0348	C20	0.072	0.014	0.043
C5	0.0456	0.0148	0.0302	O25	0.0146	0.0062	0.0104
C4	0.0413	0.0011	0.0212	O28	0.0197	0.0292	0.0245
C3	0.02	0.0088	0.0144	H(C1)	0.0282	0.0176	0.0229
C2	0.0059	0.0036	0.0048	H(C6)	0.029	0.0151	0.0221
C10	0.0097	0.0333	0.0215	H(C2)	0.0298	0.0109	0.0204
C9	0.0589	0.0171	0.038	H(C8)	0.0156	0.0078	0.0117
C8	0.0062	0.0028	0.0045	H(C12)	0.003	0.0061	0.0046
C7	0.0028	0.0013	0.0021	H(C11)	0.0115	0.0119	0.0117
C14	0.045	0.0112	0.0281	H(C11)	0.0057	0.0063	0.006
C13	0.0028	0.0091	0.006	H(C15)	0.0072	0.0185	0.0129
C12	6.00E-04	0.0021	0.0013	H(O31)	0.02	0.0069	0.0134
C11	0.0036	0.0057	0.0046	H(O29)	0.0163	0.0099	0.0131
C18	-1.00E-04	0.082	0.041	H(O32)	0.0086	0.0266	0.0176
C17	0.0046	0.0355	0.0201	H(N24)	0.0105	0.0205	0.0155
C16	0.0094	0.0866	0.048	H(N24)	0.0049	0.0074	0.0062
C15	0.0025	0.0087	0.0056	H(C21)	0.0076	0.0156	0.0116
O31	0.0992	0.0228	0.061	H(C21)	-0.0015	0.0066	0.0025
O30	0.0283	0.0407	0.0345	H(C21)	0.0089	0.0132	0.0111
O29	0.0655	0.02	0.0427	H(C22)	0.0078	0.0174	0.0126
O27	0.0092	0.0987	0.0539	50(C22)	0.0015	3.00E-04	9.00E-04
O32	0.0168	0.0565	0.0367	H(C22)	0.0078	0.0099	0.0089
C19	0.0062	0.0033	0.0047	H(C20)	0.0104	0.0112	0.0108
N24	0.0111	0.0163	0.0137	H(C20)	0.0147	0.0041	0.0094
O26	0.0321	0.0331	0.0326	H(C20)	0.0025	0.0015	0.002
N23	4.00E-04	0.0061	0.0032	H(O25)	0.0115	0.0093	0.0104
C21	0.0034	0.0103	0.0068	H(O28)	0.008	0.0086	0.0083

Tab. S2. Fukui calculation results of CIP molecular.

Atoms	$f^-(e)$	$f^+(e)$	$f^0(e)$	Atoms	$f^-(e)$	$f^+(e)$	$f^0(e)$
O22	0.0387	0.0427	0.0407	C11	0.0192	0.0737	0.0465
C14	0.0094	0.0122	0.0108	O21	0.076	0.0851	0.0805

C12	0.0209	0.0278	0.0244	O23	0.0237	0.031	0.0274
C13	0.0181	0.0059	0.012	H(C13)	0.0162	0.0345	0.0253
N20	0.0141	0.033	0.0236	H(C15)	0.0068	0.017	0.0119
C15	-0.0017	9.00E-04	-4.00E-04	H(C16)	0.0076	0.0163	0.012
C16	0.0061	0.0129	0.0095	H(C16)	0.0029	0.0067	0.0048
C17	0.0145	0.0152	0.0149	H(C17)	0.0086	0.009	0.0088
C9	0.0234	0.0138	0.0186	H(C17)	0.0142	0.0184	0.0163
C8	0.0641	0.0115	0.0378	H(C7)	0.0219	0.0297	0.0258
C7	0.0271	0.0629	0.045	H(C1)	0.0149	0.0053	0.0101
C5	0.0508	0.0389	0.0448	H(C1)	0.0262	0.0161	0.0211
F	0.0398	0.0325	0.0361	H(C2)	0.0143	5.00E-04	0.0074
C6	0.021	0.0567	0.0388	H(C2)	0.0251	0.0165	0.0208
N18	0.1003	0.0238	0.0621	H(N19)	0.0253	0.0127	0.019
C1	0.0185	0.0084	0.0135	H(C3)	0.024	0.0148	0.0194
C2	0.0193	0.0069	0.0131	H(C3)	0.014	0	0.007
N19	0.0353	0.0106	0.0229	H(C4)	0.0275	0.0177	0.0226
C3	0.0218	0.0864	0.0541	H(C4)	0.0167	0.004	0.0103
C4	0.0178	0.0071	0.0124	H(C10)	0.0155	0.0219	0.0187
C10	0.0324	0.0484	0.0404	H(O23)	0.0075	0.0107	0.0091

ETC（epitetracyclin）

Tab. S3. Potential intermediates in the TC photocatalytic degradation by H_2/T-BC.

TPs	m/z	Molecular formula	Supposed Structure	RSs/TPs Pathway	Refs.
P1	459	C22H22N2O9	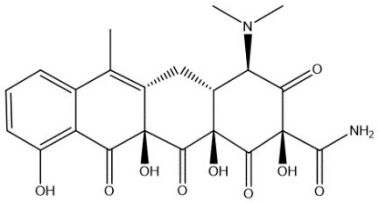	$\cdot O_2^-$/ETC Hydroxylation	11
P2	443	C22H21NO9	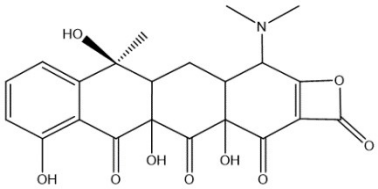	$\cdot O_2^-$/TC 1)Hydroxylation 2)Ring formation	12
P3	431	C21H22N2O8	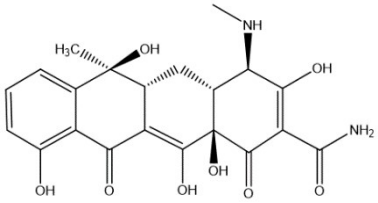	h^+/ETC Demethylation	11
P4	428	C22H21NO8	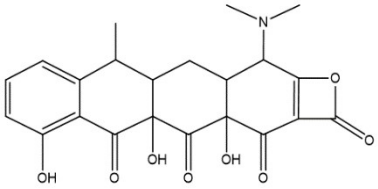	$\cdot O_2^-$/TC Hydroxylation	12
P5	427	C23H25NO7	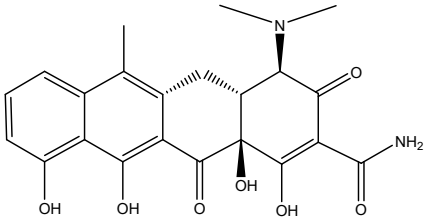	$\cdot O_2^-$/ETC Aromatization	11
P6	399	C20H18N2O7	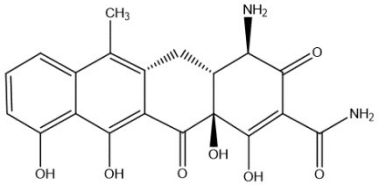	h^+/P5 Demethylation	11

P7	398	C21H19NO7	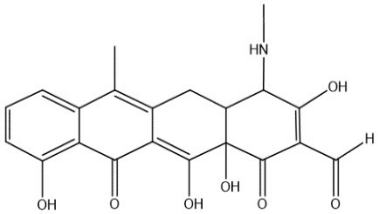	RSs/P2 Decompose	12
P9	301	C18H20O4	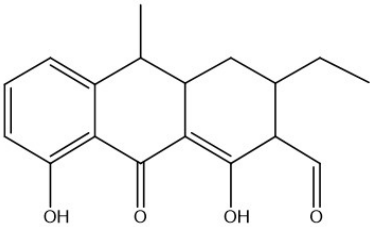	RSs/P2, P7 Disintegrated	12
P10	282	C18H18O3	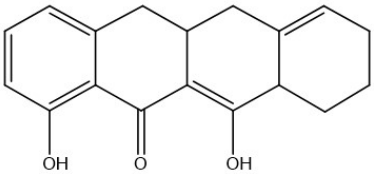	h^+ 1)Dehydroxylation 2)Demethylation	13
P11	239	C12H14O5	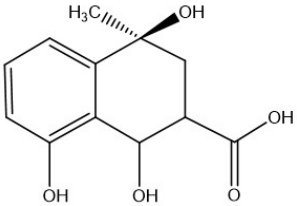	RSs/P356 Ring opening	11
P13	135	C8H6O3	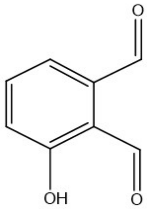	RSs/P2, P7 Disintegrated	12
P14	130	C8H18O	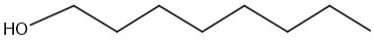	RSs/TPs The cleavage of TPs	14

Tab. S4. Potential intermediates in the TC photocatalytic degradation by H_2/T-BC under acidic conditions.

TPs	m/z	Molecular formula	Supposed Structure	RSs/TPs Pathway	Refs.
P15	324	C19H14O5	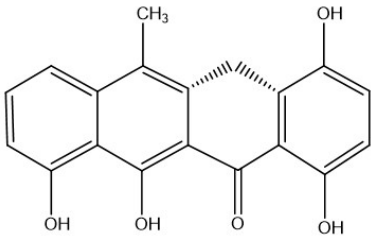	RSs/P3 5 6 Ring opening	11

Tab. S5. Potential intermediates in the TC photocatalytic degradation by H_2/T-BC under neutral conditions.

TPs	m/z	Molecular formula	Supposed Structure	RSs/TPs Pathway	Refs.
P16	417	C20H20N2O8	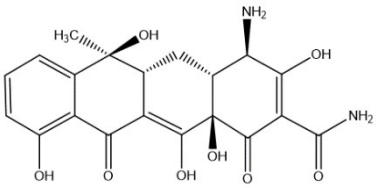	h^+/ETC Demethylation	11
P17	415	C20H18N2O8	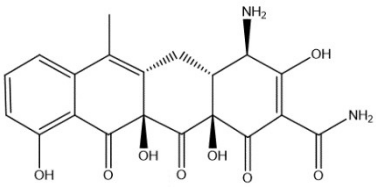	h^++·O_2^-/ETC 1)Hydroxylation 2)Demethylation	11
P18	385	C21H23NO6	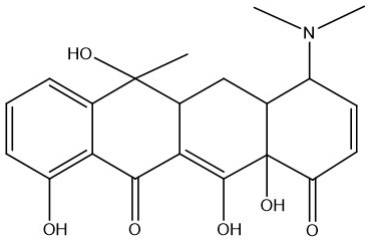	h^+ 1)Dehydroxylation 2)Demethylation	13
P15	324	C19H14O5	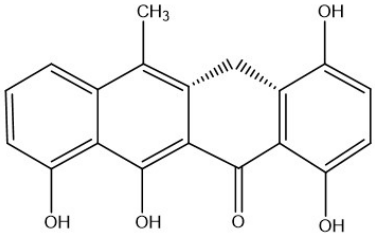	RSs/P3 5 6 Ring opening	11

P19	296	C18H17NO3	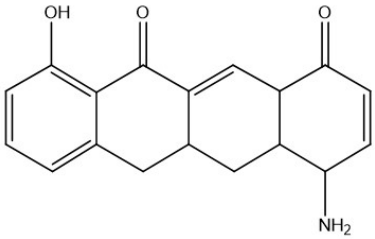	h^+/TC Detachment of functional groups of TC molecule	15
P20	136	C9H12O	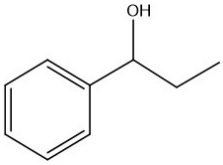	RSs/TPs The cleavage of tetracycline	14

Tab. S6. Potential intermediates in the TC photocatalytic degradation by H_2/T-BC under alkalinity conditions.

TPs	m/z	Molecular formula	Supposed Structure	RSs/TPs Pathway	Refs.
P16	417	C20H20N2O8		$h^{+/}$ETC Demethylation	11
P17	415	C20H18N2O8	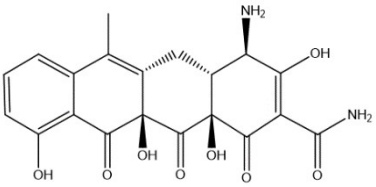	h^++·O_2^-/ETC 1)Hydroxylation 2)Demethylation	11
P21	410	C22H21NO7	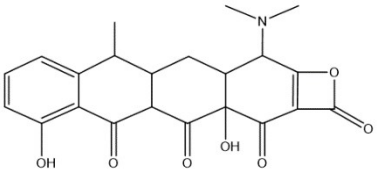	h^+/P4 Dehydroxylation	12
P18	385	C21H23NO6		h^+ 1)Dehydroxylation 2)Demethylation	13

P19	296	C18H17NO3		h^+/TC Detachment of functional groups of TC molecule	15
P20	136	C9H12O		RSs/TPs The cleavage of tetracycline	14

Tab. S7. Potential intermediates in the CIP photocatalytic degradation by H_2/T-BC.

TPs	m/z	Molecular formula	Supposed Structure	RSs/TPs Pathway	Refs.
P1	362	C17H16FN3O5	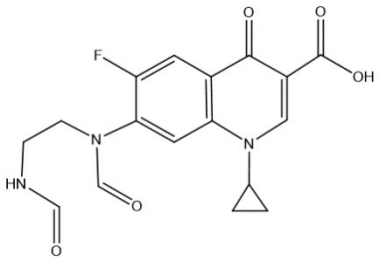	RSs/CIP 1)The cleavage of the piperazine ring 2)With two keto-groups on the piperazine ring	16
P3	263	C13H11FN2O3	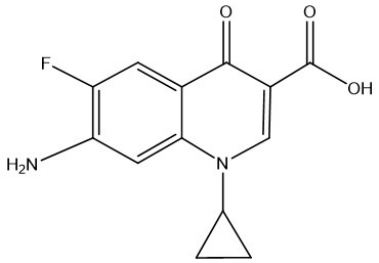	RSs/P1 Detachment of functional groups of CIP molecule	16

Tab. S8. Potential intermediates in the CIP photocatalytic degradation by H_2/T-BC under acidic conditions.

TPs	m/z	Molecular formula	Supposed Structure	RSs/TPs Pathway	Refs.

P4	334	C16H19N3O5	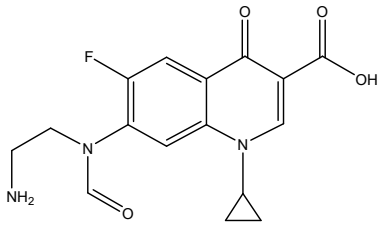 or 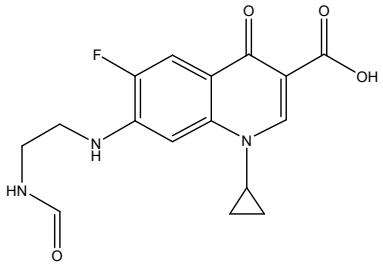	$h^{+}+{}^{1}O_2$/P1 Decarbonylation	17

Tab. S9. Potential intermediates in the CIP photocatalytic degradation by H_2/T-BC under neutral conditions.

TPs	m/z	Molecular formula	Supposed Structure	RSs/TPs Pathway	Refs.
P5	344	C17H17N3O5	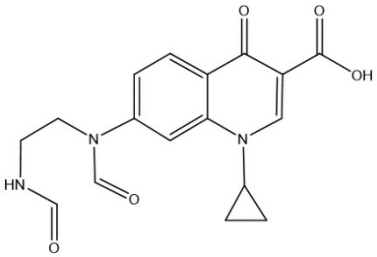	$h^{+}+{}^{1}O_2$/CIP 1)The cleavage of the piperazine ring 2)Defluorination	18
P6	316	C16H17N3O4	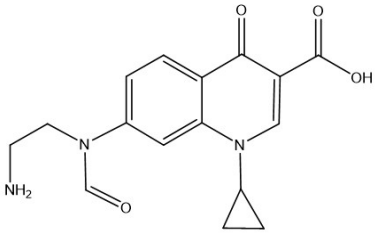	h^{+}/P6 Decarbonylation	18
P7	330	C17H19N3O4	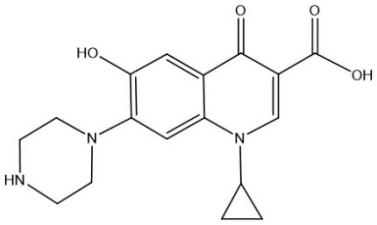	$h^{+}+\cdot O_2^{-}$/CIP 1)Defluorination 2)Hydroxylation 3)Dehydroxylation	18

P8	288	C15H17N3O3	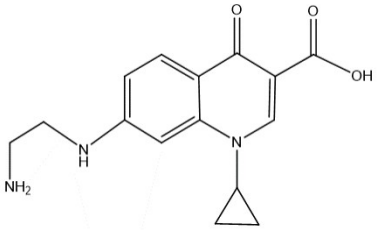	$h^+ + {}^1O_2$/P7 Decarbonylation	18

Tab. S10. Potential intermediates in the CIP photocatalytic degradation by H_2/T-BC under alkalinity conditions.

TPs	m/z	Molecular formula	Supposed Structure	RSs/TPs Pathway	Refs.
P9	348	C17H18FN3O4	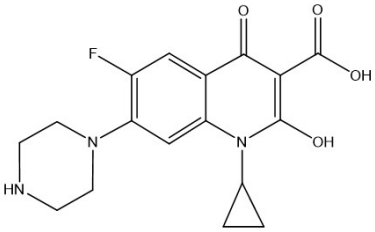	$\cdot O_2^-$/CIP Hydroxylation	16
P7	330	C17H19N3O4		$h^+ + \cdot O_2^-$/CIP 1)Defluorination 2)Hydroxylation 3)Dehydroxylation	18
P6	316	C16H17N3O4	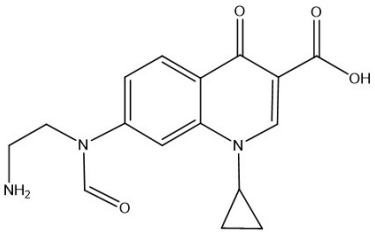	$h^+ + {}^1O_2$/P1 1)Defluorination 2)Decarbonylation	18
P10	306	C15H16N3O3F	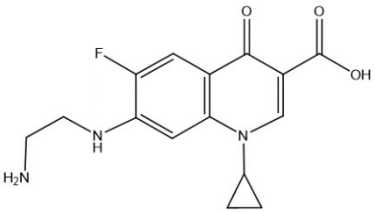	$h^+ + {}^1O_2$/P1 Decarbonylation	16

P11	291	C14H11FN2O4	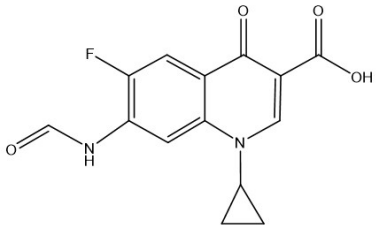	h^+/P11 The cleavage of the piperazine ring	17
P8	288	C15H17N3O3	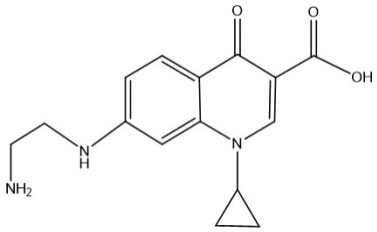	h^+/P11 Defluorination	18
P12	280	C14H18N3O2F	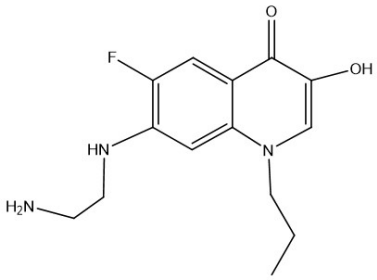	h^++$^1O_2$/P11 piperazine ring and cyclopropyl were broken	17

Tab. S11 Contribution rates of active species for organic pollutants degradation.

		pH	k	Contribution rate%		pH	k	Contribution rate%
TC	-	3	0.01218	100	CIP	3	0.00135	100
		7	0.01296	100		7	0.00927	100
		10	0.00949	100		10	0.1027	100
	EDTA-2Na	3	0.01218	98.36		3	0.00135	92.59
		7	0.01296	82.25		7	0.00927	94.61
		10	0.00949	94.73		10	0.1027	99.61
	KBrO3	3	0.01218	80.30		3	0.00135	11.11
		7	0.01296	77.62		7	0.00927	21.25
		10	0.00949	32.56		10	0.1027	71.76
	TBA	3	0.01218	96.72		3	0.00135	77.78
		7	0.01296	45.99		7	0.00927	13.70
		10	0.00949	37.83		10	0.1027	64.95
	P-BQ	3	0.01218	98.36		3	0.00135	77.78
		7	0.01296	59.10		7	0.00927	24.49
		10	0.00949	62.07		10	0.1027	97.08
	DABCO	3	0.01218	53.20		3	0.00135	62.96
		7	0.01296	46.76		7	0.00927	97.84
		10	0.00949	34.67		10	0.1027	99.03

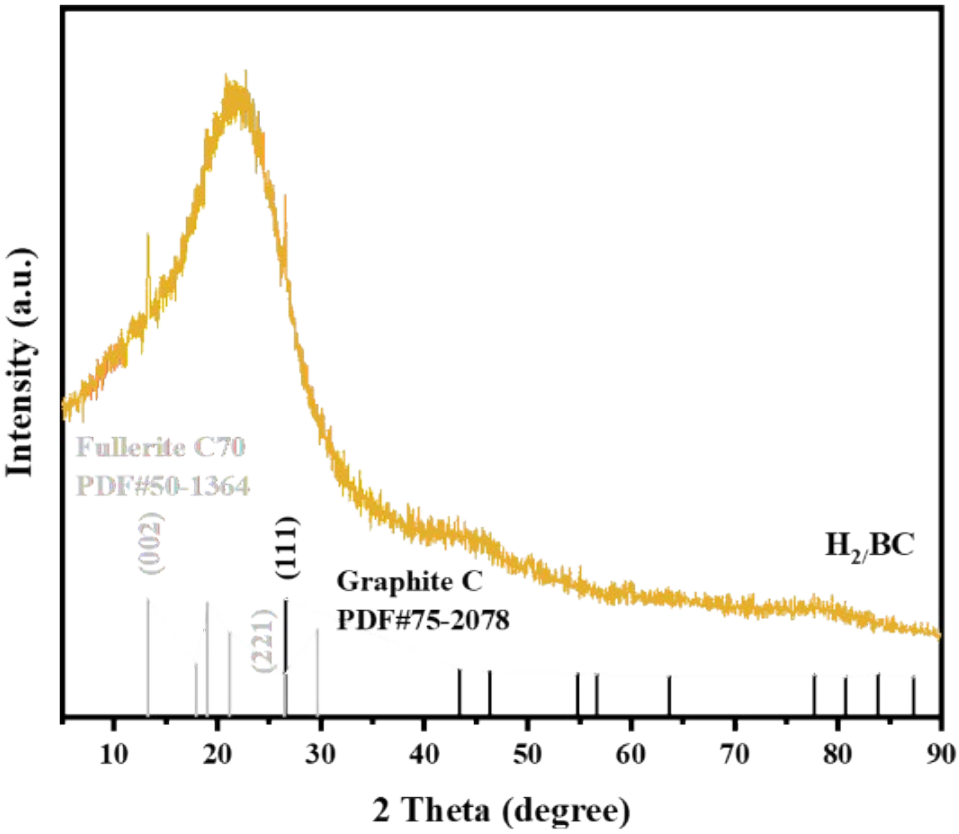

Fig. S1. XRD of H_2/BC.

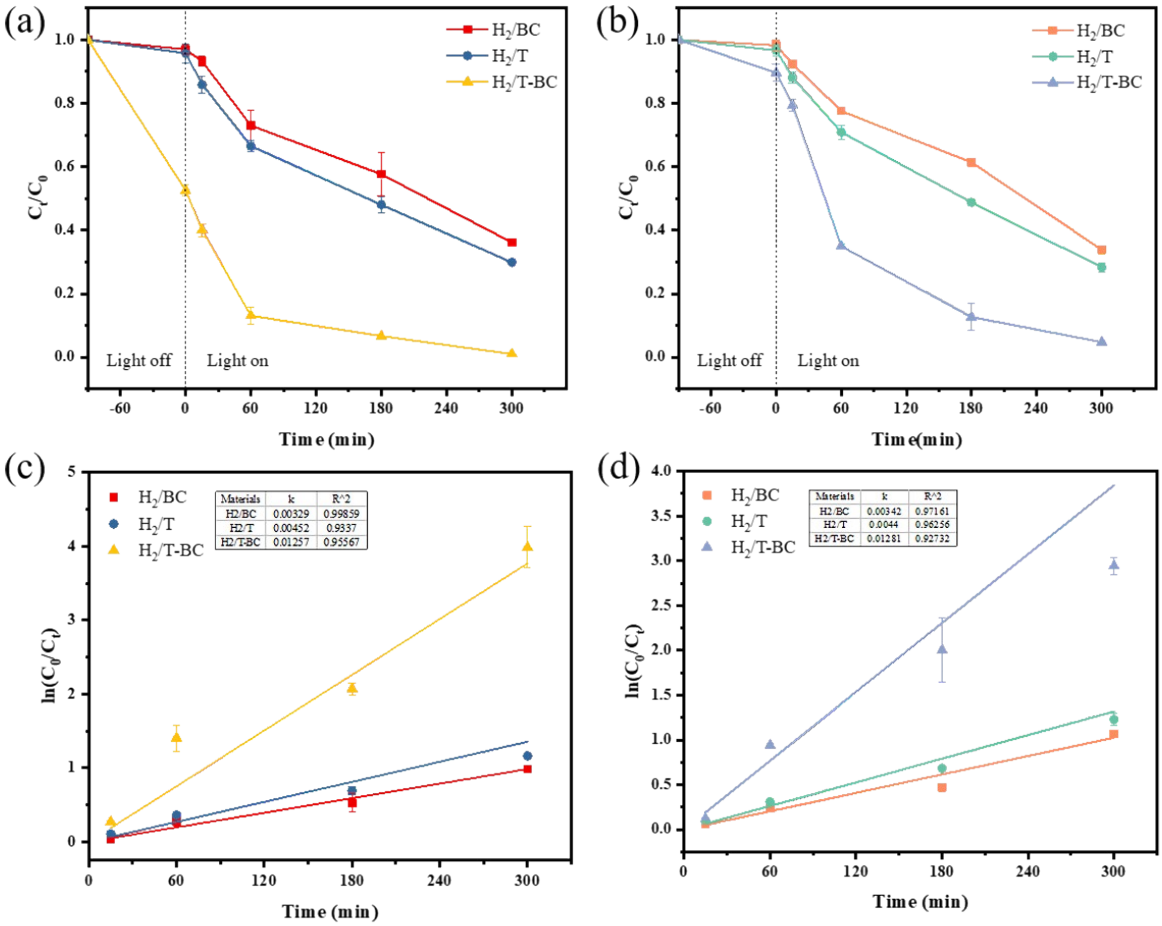

Fig. S2. Effect of different materials on degrading (a) TC, (b) CIP, and the reaction rate of (c)TC, (d) CIP.

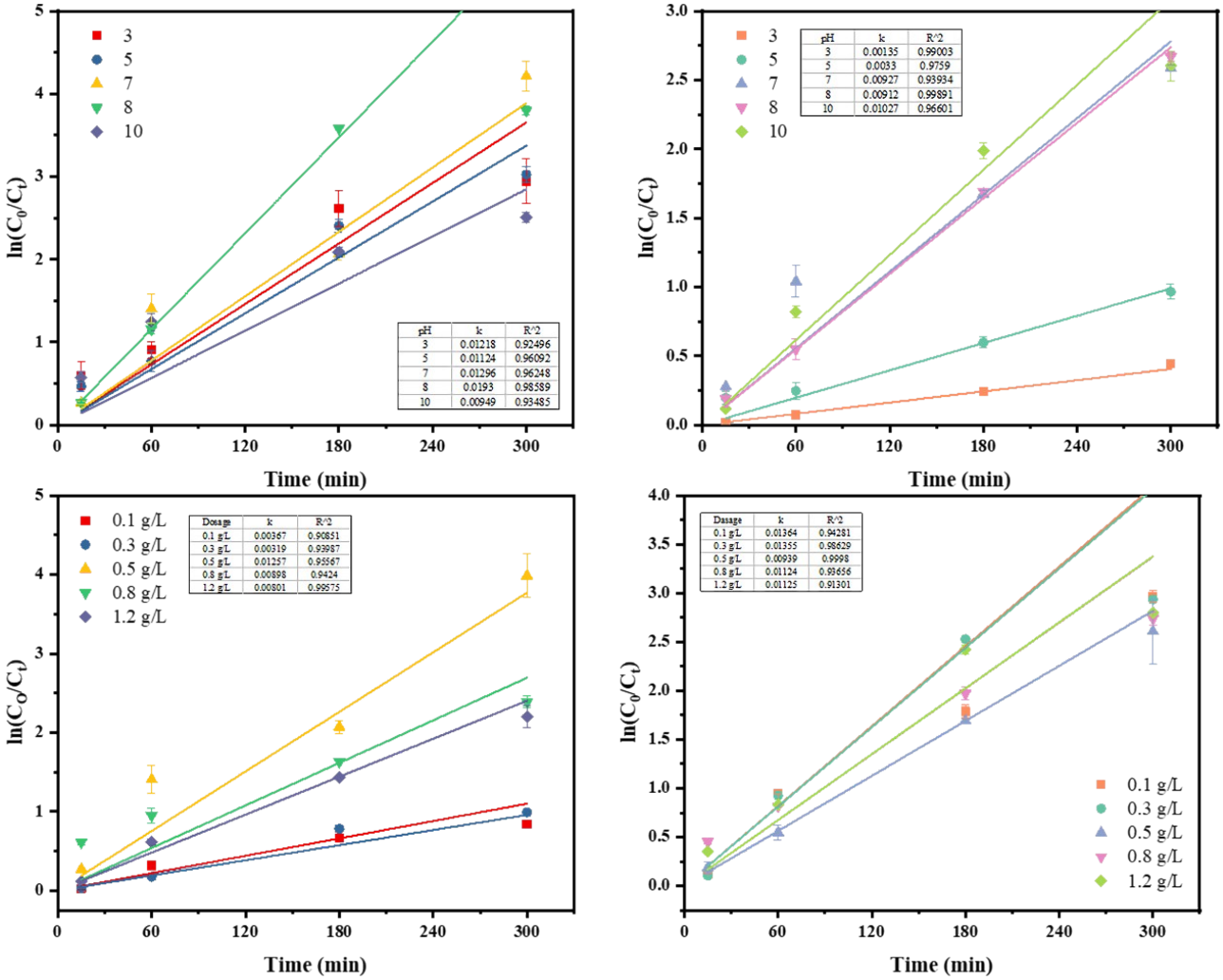

Fig. S3. The reaction rate of (a) TC, (b) CIP at different pH, and (c)TC, (d) CIP at different dosages of H_2/T-BC.

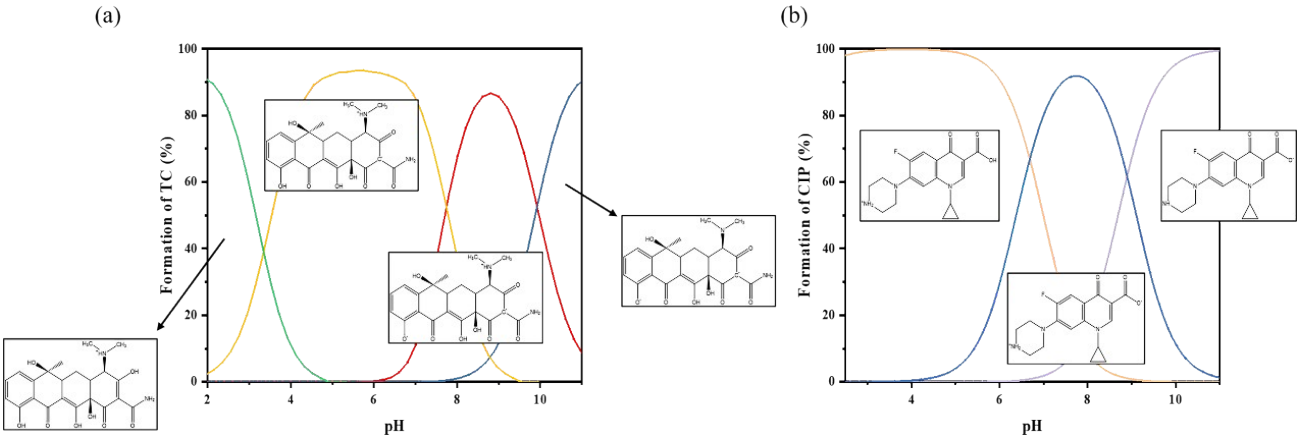

Fig. S4. The pKa of (a) TC and (b) CIP: The surface charge of antibiotics under different pH conditions.

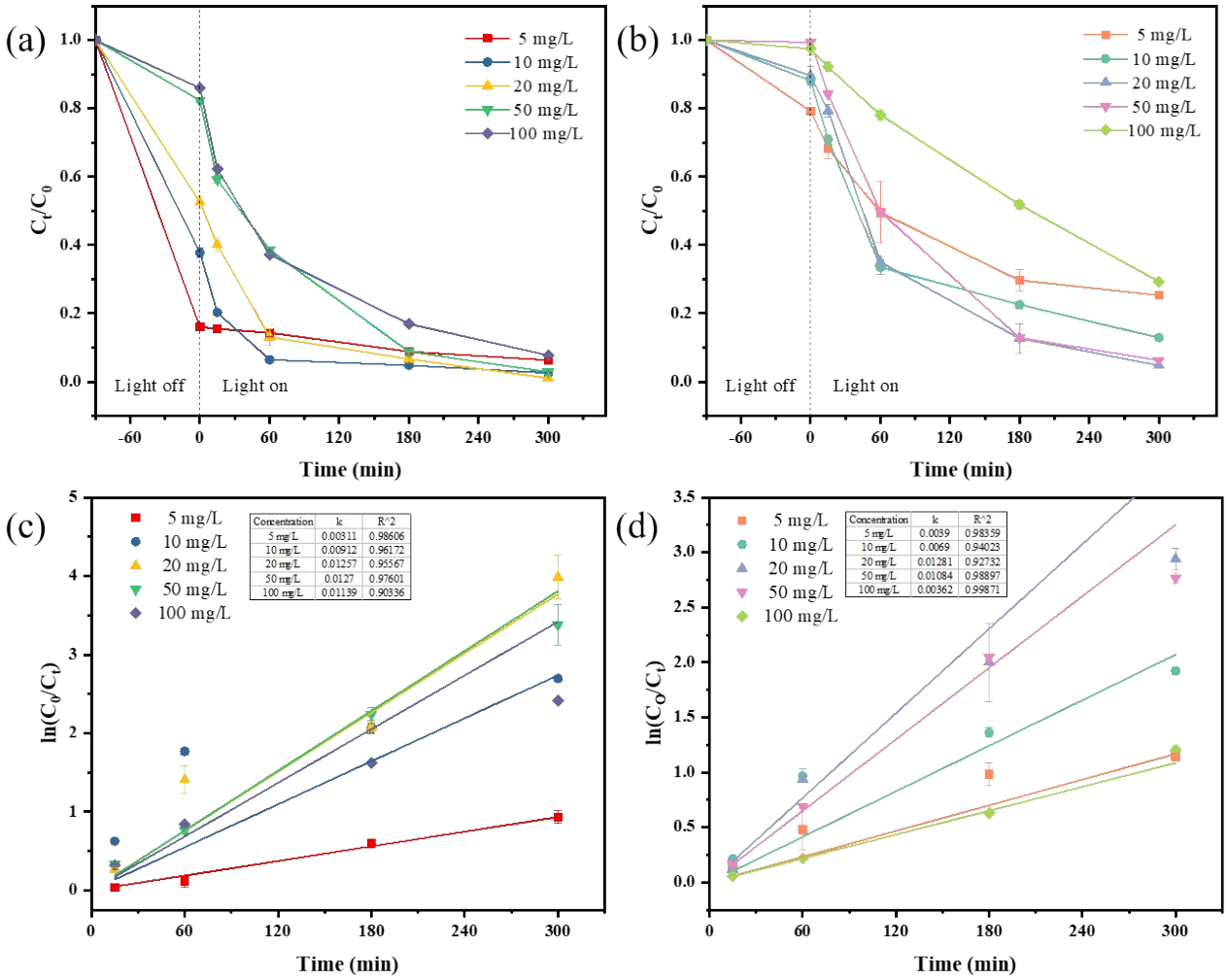

Fig. S5. Degradation of (a) TC, (b) CIP at different initial concentrations, and the reaction rate of (c)TC, (d) CIP.

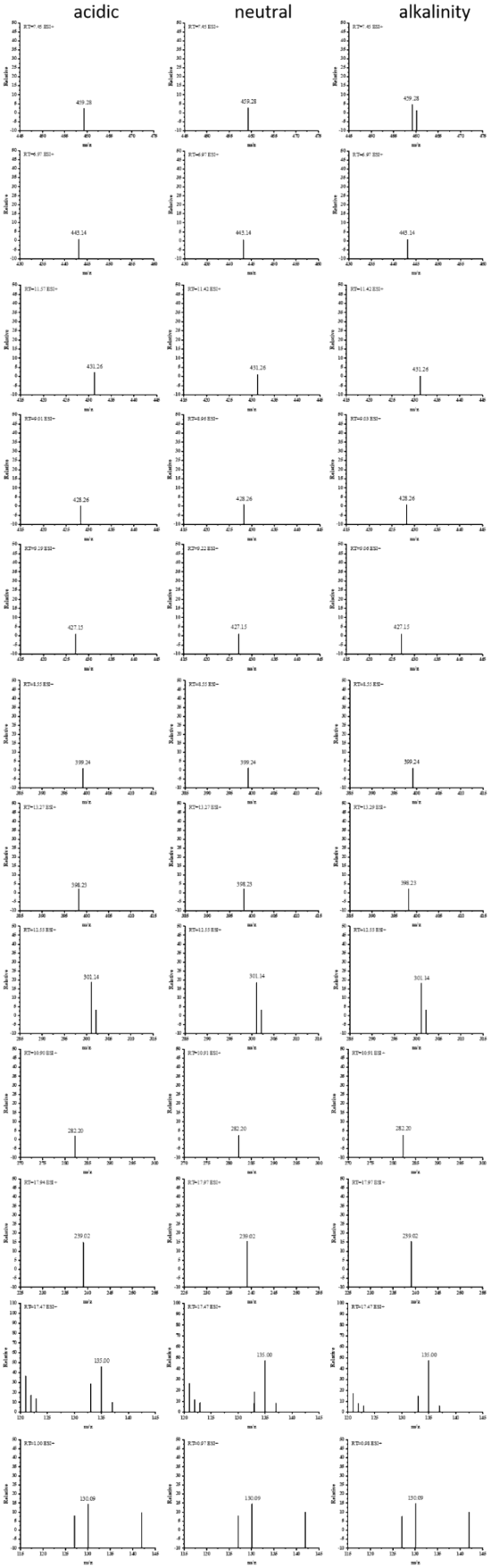

Fig. S6. MS^2 spectra of intermediate products resulting from TC photocatalytic degradation

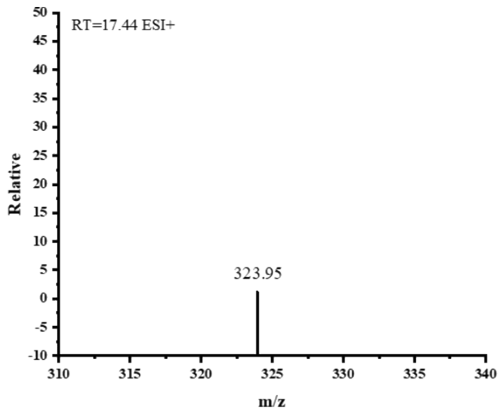

Fig. S7. MS^2 spectra of intermediate products resulting from TC photocatalytic degradation under acidic conditions.

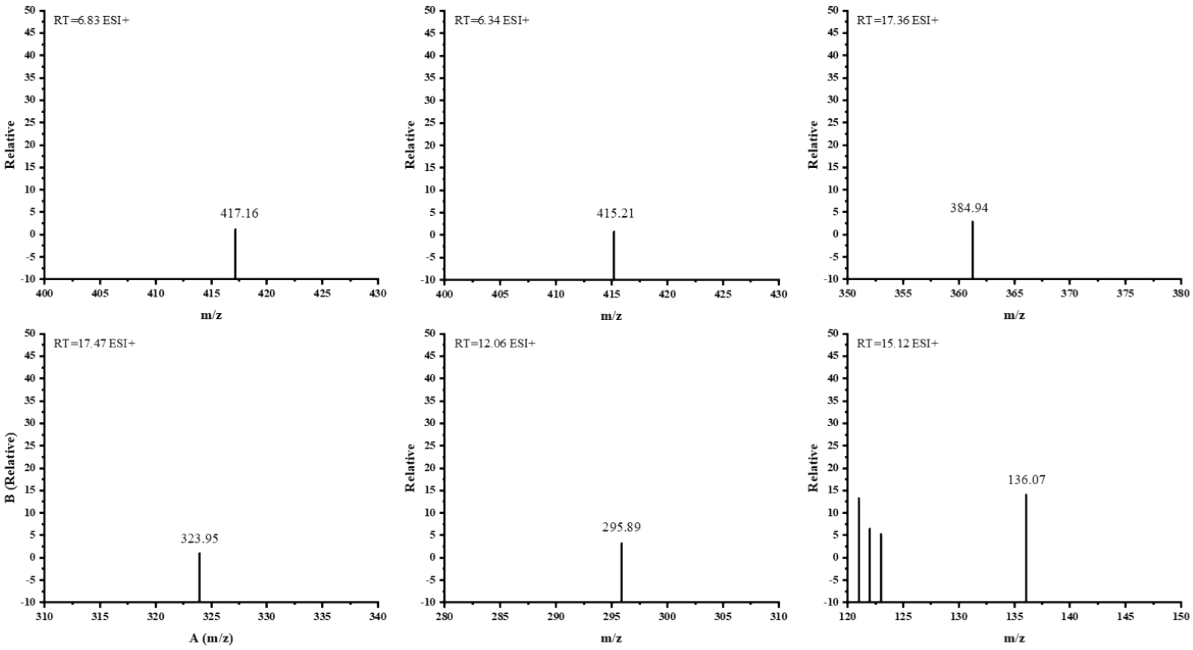

Fig. S8. MS^2 spectra of intermediate products resulting from TC photocatalytic degradation under neutral conditions.

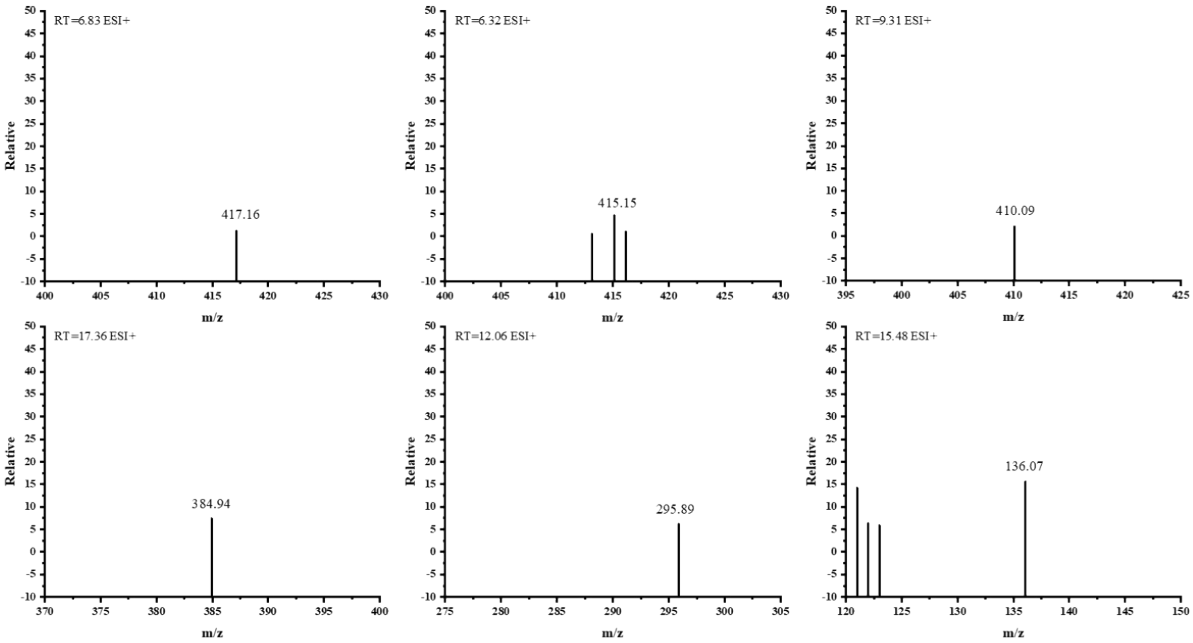

Fig. S9. MS^2 spectra of intermediate products resulting from TC photocatalytic degradation under alkaline conditions.

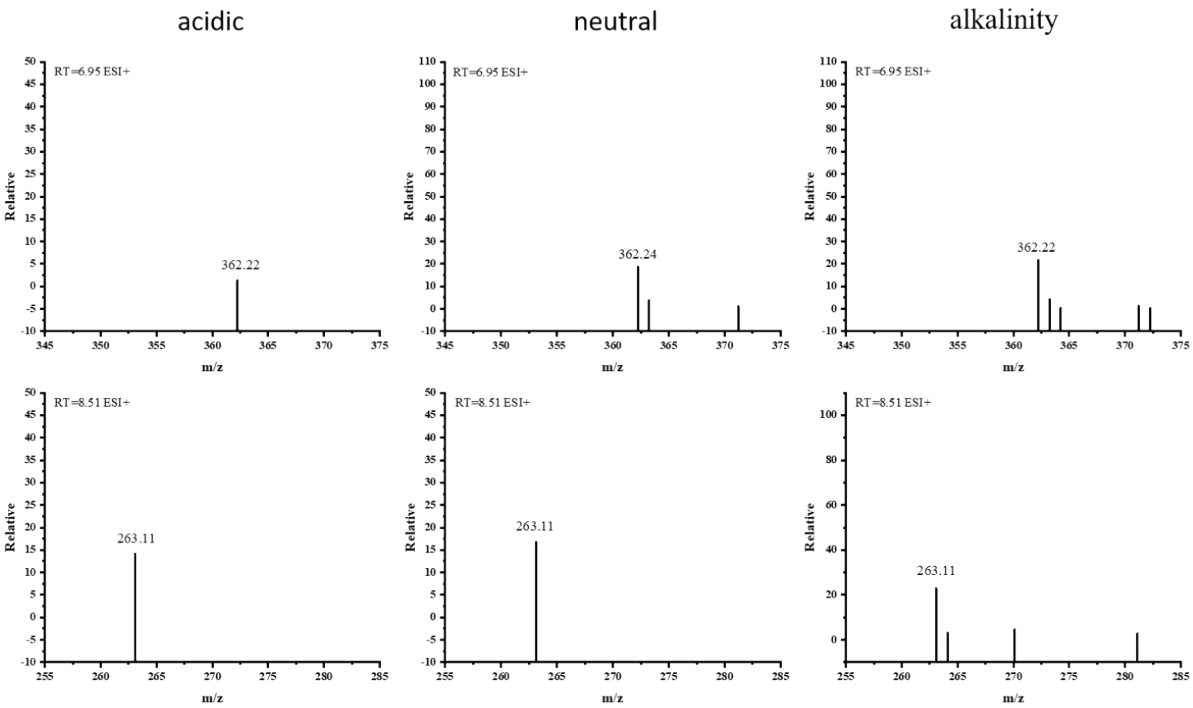

Fig. S10. MS^2 spectra of intermediate products resulting from CIP photocatalytic degradation

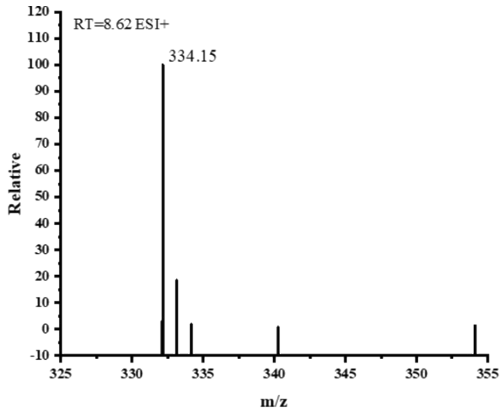

Fig. S11. MS^2 spectra of intermediate products resulting from CIP photocatalytic degradation under acidic conditions.

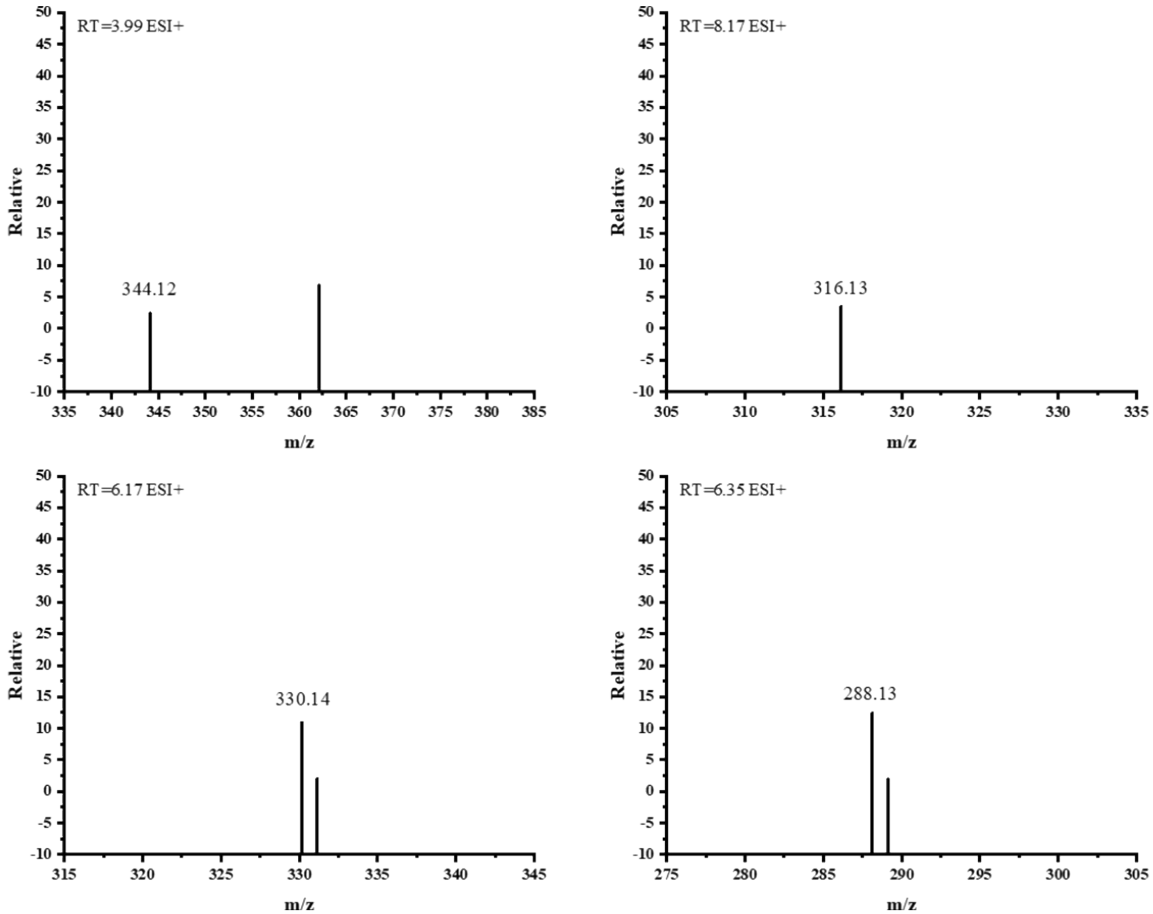

Fig. S12. MS^2 spectra of intermediate products resulting from CIP photocatalytic degradation under neutral conditions.

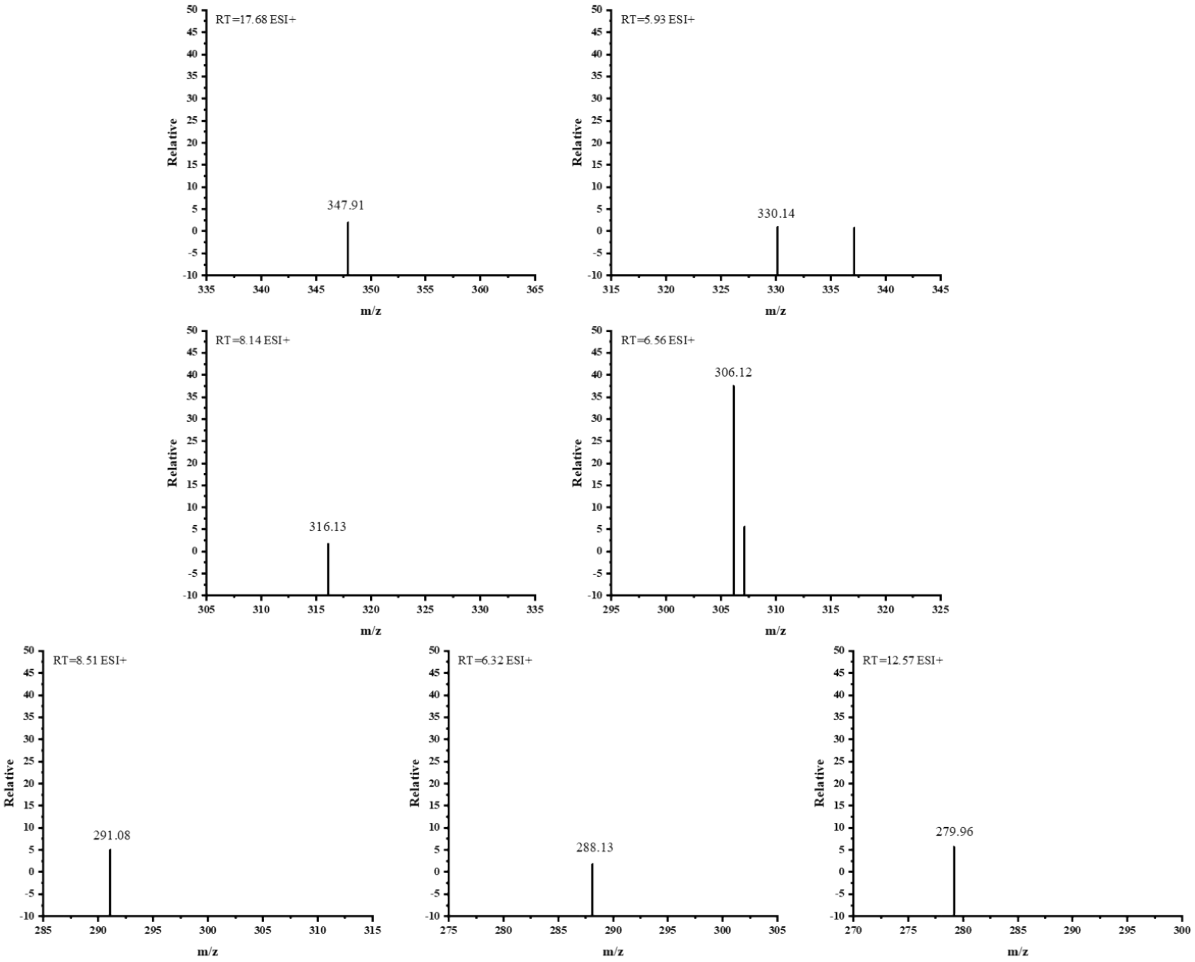

Fig. S13. MS^2 spectra of intermediate products resulting from CIP photocatalytic degradation under alkaline conditions.

References

1. J. Tauc, *Journal*, 1972.
2. G. Jia, Y. Wang, X. Cui and W. Zheng, *ACS Sustainable Chemistry & Engineering*, 2018, **6**, 13480-13486.
3. T. T. a. A. ISHITANI, *Carbon*, 1984, **22**, 43-46.
4. M. Smith, L. Scudiero, J. Espinal, J.-S. McEwen and M. Garcia-Perez, *Carbon*, 2016, **110**, 155-171.
5. T. A. Gad-Allah, M. E. Ali and M. I. Badawy, *J Hazard Mater*, 2011, **186**, 751-755.
6. T. An, H. Yang, G. Li, W. Song, W. J. Cooper and X. Nie, *Applied Catalysis B: Environmental*, 2010, **94**, 288-294.
7. R.-y. Zhou, J.-x. Yu, H.-x. Li and R.-a. Chi, *Colloids and Surfaces A: Physicochemical and Engineering Aspects*, 2020, **603**.
8. J. X. Yu, J. Zhu, L. Y. Feng and R. A. Chi, *J Colloid Interface Sci*, 2015, **451**, 153-160.
9. Z. Zhang, L. Moghaddam, I. M. O'Hara and W. O. S. Doherty, *Chemical Engineering Journal*, 2011, **178**, 122-128.
10. T. E. Abilio, B. C. Soares, J. C. Jose, P. A. Milani, G. Labuto and E. Carrilho, *Environ Sci Pollut Res Int*, 2021, **28**, 24816-24829.
11. Q. Zhang, L. Jiang, J. Wang, Y. Zhu, Y. Pu and W. Dai, *Applied Catalysis B: Environmental*, 2020, **277**.
12. Q. Si, W. Guo, H. Wang, B. Liu, S. Zheng, Q. Zhao, H. Luo, N. Ren and T. Yu, *Applied Catalysis B: Environmental*, 2021, **299**.
13. L. Qin, Z. Wang, Y. Fu, C. Lai, X. Liu, B. Li, S. Liu, H. Yi, L. Li, M. Zhang, Z. Li, W. Cao and Q. Niu, *J Hazard Mater*, 2021, **414**, 125448.
14. V. H. Tran Thi and B. K. Lee, *J Hazard Mater*, 2017, **324**, 329-339.
15. Y. X. Pang, L. J. Kong, H. Y. Lei, D. Y. Chen and G. Yuvaraja, *JOURNAL OF THE TAIWAN INSTITUTE OF CHEMICAL ENGINEERS*, 2018, **93**, 397-404.
16. K. Hu, R. Li, C. Ye, A. Wang, W. Wei, D. Hu, R. Qiu and K. Yan, *Journal of Cleaner Production*, 2020, **253**.
17. F. Wang, X. Yu, M. Ge and S. Wu, *Chemical Engineering Journal*, 2020, **384**.
18. A. Salma, S. Thoroe-Boveleth, T. C. Schmidt and J. Tuerk, *J Hazard Mater*, 2016, **313**, 49-59.